M. C. Evernden and J. T. MOTTRAM, 'Closed-form equations for flange force and maximum deflection of box-beams of fiber reinforced polymer with partial shear interaction between webs and flanges,' *Advances in Structural Engineering*, **14** 6, (2011), 991-1004. ISSN 1369-4332

Closed-form equations for flange force and maximum deflection of box-beams of fiber reinforced polymer with partial shear interaction between webs and flanges

M. C. Evernden[1] and J. T. Mottram[2]

Abstract

Presented in the paper is the formulation of a governing second-order differential equation for the moment distribution along the length of a beam having two interfaces with partial shear interaction where two flange and two web components join to form the box shaped section. For practical applications such a closed-section beam of Fiber Reinforced Polymer (FRP) can be assembled from individual pultruded profiles using mechanical fasteners. This assembly approach can be used to construct deeper section sizes than can be achieved with a single pultrusion, and which can be transported in flat-pack units. In developing the governing equation for flexural response account is made of the finite connection stiffness at the web/flange interfaces by applying conventional elastic beam theory. The differential equation for the partial interaction problem is solved to formulate closed form equations for the flange force and the maximum deflection of a simply supported beam under four-point bending. A numerical parametric study is presented to show changes in beam performance indicators with the degree of shear interaction between the upper and lower bounds of full- and non-interaction. Results from a series of load tests using a three-layered prototype FRP beam are shown to be in good agreement. The theoretical predictions for maximum deflection are however found to be directly linked to the appropriateness of the measured connection stiffness entered into the closed-form equation.

Key words: Pultruded FRP beam, deflection, theoretical analysis

[1]Lecturer, School of Architecture and Civil Engineering, University of Bath, E-mail: M.Evernden@bath.ac.uk

[2]Reader, School of Engineering, University of Warwick, Coventry, CV4 7AL, UK. E-mail: J.T.Mottram@warwick.ac.uk

1.0 Introduction

Pultrusion is an economical process for Fibre Reinforced Polymer (FRP) material that produces profiles of E-glass fibre and, often, a matrix of polyester or vinyl ester resin (Anon, 2010a; Anon, 2010b). Profiles are thin-walled and prismatic, and standard (structural) profiles mimic those sections used in steelwork (Bank, 2006). The largest stocked pultrudate of I-shape is 360 mm deep, 180 mm wide, and has 12.7 mm thick walls. Being lightweight and resistant to corrosion pultruded Fiber Reinforced Polymer (FRP) profiles are used in construction applications when their property portfolio adds value to the engineered solution. Larger sized I- and H-shaped profiles are available only to order, and the American pultruder Strongwell offers a I-profile of size 609 x 9.53 x 190.5 x 19.05 mm (24 x 3/8 x 7.5 x 3/4 in.), having a second moment of area about the major axis of 7.9×10^{-4} m^4. For a span to depth ratio of 12 a simply supported beam of this beam profile can carry a uniformly distributed load of 5 kN/m for an initial mid-span deflection of span/360. Because there is not an extensive range of standard profiles to choose from (see Anon, 2010a; Anon 2010b; Anon 2010c), the next down in size has a second moment of area only 28% of the maximum. In response to this limitation, and specifically for simply supported bridge girder applications (and without composite action with the road deck), Strongwell developed a non-standard double web profile (Anon, 2003), having a second moment of area eight times the largest I-section size. This unique pultruded profile (envelop is 914 x 907 mm (36 x 18 in.)) has an even higher relative flexural rigidity because the fiber reinforcement is a hybrid of E-glass and a higher modulus carbon.

Given the choice limitation imposed by the current available range in standard profile shapes and sizes, and recognizing that, when compared to the open-sections, a closed box-section shape gives superior structural properties other approaches to achieving second moment of areas > 7.9×10^{-4} m^4 are attractive. This paper presents a partial interaction analysis for one promising approach that uses two identical flange profiles and two identical web profiles to assemble a box-shaped beam from four pultruded

FRP components. Figure 1 shows an experimental beam, based on this 'flat-pack' concept, which is 400 mm deep. It is fabricated from four thin-walled components that are connected along their full lengths with mechanical ('blind') fasteners. As Figures 1(a) and 1(b) show the two webs are 380 mm deep and have a nominal wall thickness of 6.4mm. The webs were cut from standard flat sheet material (Series 1625) supplied by the American pultruder Creative Pultrusions Inc. Although the depth of web can be changed it is envisaged that there is only to be one size of flange profile, comprising of the flange panel with two outward facing channels that will accept the blind fixings to assemble the box-section. For the test beam in Figure 1(a-b), Figure 1(c) shows that the flange is 203 x 9.53 mm (8 by 3/8 in.) and that the pultruded channel is for the M10 size of Unistrut connector. To fabricate the test beam the flange panel was cut from a standard wide-flange section (Series 1525) of 203 x 203 x 9.5 mm (8 x 8 x 3/8 in.) from Creative Pultrusions Inc. and adhesively bonded (toughened epoxy) to specialized Unistrut channels pultruded by Fibreforce Composites, UK (now part of EXEL Composites). As can be seen in Figures 1(a) to 1(c) the web and flange components are joined together with four rows (there are two rows for the rear web not in view) of the Unistrut connectors that can be individually spaced at 50 mm along the complete length of the assembly. Each mechanical fastener is a Unistrut connector with its M10 bolt installed through a 10.5 mm diameter hole and subjected to a tightening torque of 20 Nm. In the PhD thesis by the first author (Evernden, 2006) the specimen in Figure 1(a) is referred to as the 'prototype beam'. We shall use this descriptor in the remainder of the paper.

The method of connection for the prototype beam uses the M10 Unistrut connector shown in Figure 1(d). It comprises a nut with a spring on one side. To insert the nut into its channel, as shown in Figure 1(b), its longer sides are aligned with the channel's opening. The nut is then pushed into the opening so that the spring is fully compressed. Rotating the nut through 90° and releasing the pressure allows the spring to uncoil and the two lips of the channel seen in Figure 1(b) mated with the matching ribbed-grooves in the nut (Figure 1(d)). The recoiled compressed spring provides sufficient pre-load to prevent the connector from moving in the channel while a M10 steel bolt is pushed through the hole in the adjoining plate, threaded into the nut and tightened to the required bolt torque. The Unistrut connector provides a quick and simple connection method for blind fixings. Whilst method of connection is common

in the metal framing industry it can also be used with FRP materials through the specific pultruded channel profile seen in Figures 1(b) and 2(a).

Under the action of shear force it can be expected that there will be some give within this mechanical fastening and so it is necessary to know the connector's shear stiffness when we account for partial shear interaction in beams deforming under vertical loading. Evernden and Mottram (2006) used a non-standard pull-out test method to determine the shear force-slip behaviour of the M10 Unistrut in its specific pultruded FRP channel. The specimen, with back-to-back channels bonded together, is shown on its own in Figure 2(a) and in the load testing machine in Figure 2(b). Tensile loading is applied using a constant stroke rate of 0.3 mm/s and the slip between connector and channel was taken to be the stoke displacement recorded by the testing machine (Evernden and Mottram, 2006). Figure 2(c) shows a typical plot of the force (kN) against slip (mm) and the linear curve to a slip of 0.5 mm that is used to characterise the constant connection stiffness for the test conditions employed.

The prototype beam assembly introduced above has been thoroughly studied through a series of four-point bending load tests and the test results and findings are fully reported in Evernden (2006). Later in this paper results from the test programme will be compared with numerical predictions using new closed-form equations derived to take account of the partial interaction at the two planes with the shear connectors.

Because the prototype beam has connector interfaces at the top and the bottom, where the flanges and webs join, it consists of three distinct layers. To derive a closed form solution for deflection requires the development of a modified Newmark method analysis, based on the seminal work of Newmark, Siess and Viest (1952). In what follows the theoretical treatment will be presented, and new expressions for the resultant flange force and maximum mid-span deflection will be obtained for the case of four-point bending. A parametric study is presented to show the performance of the new deflection equation in terms of changing the relative shear stiffness given by the method of connection.

For a box-beam comprising two or more longitudinal components, which are joined along their lengths, a state of full-interaction (no relative slip between these individual

components) gives the section its maximum flexural rigidity. A state of non-interaction will exist if the connections exhibit zero shear stiffness and the assembly acts as individual elements bending around their own neutral axes. When components are joined together using a method of connection with finite shear stiffness a state approaching full-composite action (Johnson, 2004) is rarely achieved and the deflection response of the beam lies between the upper and lower bound limits of full- and non-interaction, respectively.

Under the more common state of partial interaction the strain difference *e*, and the associated relative slip, *s*, between the connected components has to be taken account of when formulating expressions to calculate the deflection under service loading (Oehlers and Bradford, 1995), and the strain profile through the depth of the section cannot be determined simply from knowledge of the bending moment distribution alone (Yam, 1981).

The first theoretical model for the partial shear interaction response of a two-layered beam was published in 1952 by Newmark, Siess and Viest, following the need to establish the deformation response of T-beams consisting of a steel girder and a concrete slab connected by shear studs (Yam, 1981; Johnson, 2004). Owing to the more recent application of bonding plates or strips of FRP (often with carbon fibers) to strengthen existing structures contributions to the partial interaction problem have been made in order to analysis the effect of bond-slip behavior (Rasheed and Pervaiz 2002; Lee *et al*., 1999).

Previous theoretical work, when the method of connection is by individual mechanical fasteners, has had two distinct solid layers with the ‘shear’ connectors providing relatively high level of shear stiffness. Stiffness values in the range 33-97 kN/mm at ultimate failure have been reported for combinations of through deck welded studs and profiled sheeting with concrete slab (Mottram and Johnson, 1990). In this paper new closed form expressions are developed for the analysis of box-section beams of FRP, having three-layers and two interfaces with metallic (M10 Unistrut) connectors that possess relatively a much lower relative level of shear stiffness per unit length.

2.0 Development of a modified three-layered Newmark solution

In order to analyze the three-layered system for the partial interaction problem it is necessary to modify the solution for two-layers given by Newmark *et al*. (1952). It is convenient in the theoretical treatment to let the bending moment at a section be the resultant of sectional forces acting on the individual beam (web and flange) components. This modeling simplification is shown in Figure 3, which also defines the variables that appear in the analytical treatment. Note that the depth of the two parallel webs is less than the height of the cross-section H, but this need not be adhered to. In Figure 3(a) the beam's cross-section is shown. Its two flanges are to be identical in shape and size, each having thickness d and cross-sectional area A_f. For the four-point bending arrangement shown in Figure 1 (Evernden 2006), the top flange is the one in tension and the bottom is in compression, and this gives the resultant flange couple (F ($H - d$)) illustrated by the model in Figure 3(d).

To formulate the governing second-order differential equation the following assumptions are made:

- Discretely spaced shear connectors can be replaced, over the length of the beam, by an equivalent continuous medium with a linear elastic response (constant shear stiffness) when subjected to longitudinal shear force.
- The affect of frictional force at the interfaces does not provide a contribution to the shear stiffness of the method of connection.
- Shearing deformation can be ignored so that sections initially plane, remain plane after bending. The strain distribution apposing the bending moment $M(x)$ therefore varies linearly through the depth, as illustrated by the separated parts in Figures 3 (b) and 3(c).
- There is no vertical separation between the flange and web components; there is full displacement continuity along the four interfaces that possess partial shear interaction.

When establishing the total deflection it shall be necessary to add to the bending deformation the deflection contribution due to shear deformation. Because the presence of shear deformation has no influence on how the three-layered beam responds to flexure it is not considered in the analytical treatment leading to Equation

(27). The deflection determined from using this expression is therefore only for the bending contribution. To form Equation (28) for the total vertical deflection the standard shear deformation term from Timoshenko's beam theory (Timoshenko, 1955) for the case of four-point bending is added.

Two assumed strain distributions through the depth of the box-beam section are shown in Figures 3(b) and 3(c). The first of these figures shows the actual strain condition for a state of partial interaction. For the same curvature k the distribution can be assumed to be equal to the combination of the deformation occurring when there is no interaction (this is Figure 3(c)), and a uniform strain distribution through flange depth d, from the resultant flange forces F, which is shown in Figure 3(d).

In Figure 3(a) the two distances d^* are from the upper and lower outer flange surfaces to the level of the interface plane with the web/flange connectors. The value of d^* is not necessarily equal to the distance from the upper (or lower) outer flange surfaces to the plane where the resultant flange force (F) acts. This force is known as the longitudinal shear force and is the force (i.e. the longitudinal shear force) that must be resisted by the mechanical fasteners joining the webs and flanges together. The couple generated from the existence of the two Fs is sufficient to impose the state of partial interaction in the box-beam assembly.

Because the modeling does not allow for vertical separation at an interface, the curvature k, for elastic deformation, does not change with depth y, and so the classical flexural expression $M(x)/EI$ (= k) remains valid. As Figure 3(b) shows y is taken to be the distance from the neutral axis. $M(x)$ is the bending moment distribution at a distance x from the left hand end, and the product EI is the section flexural rigidity based on the major second moment of area and longitudinal modulus of elasticity, which are both assumed to be constant along the span. Flexural rigidity has limits EI_{full} and EI_{non} for the full- and non-interaction conditions described in the previous section.

In accordance with Euler-Bernoulli beam theory when the bending moment is a function of x so must the curvature vary likewise. As Figure 3(b) shows the strain distributions through the depth of the web and the flange components are linear, but

offset. The neutral axis for the web is at its mid-depth, because the beam section is symmetrical for major-axis flexure. In Figure 3(b) n_1 is for the distance from the outer surface of the flange to where the flange strain distribution is theoretically taken to be zero. As shown in Figure 3(b) the presence of the partial interaction offsets the strain distribution for webs and flange sections horizontally giving rise to a strain difference e at the interface between the flanges and webs.

The resultant force F in a flange, can be expressed by

$$F = kE_{\mathrm{f}}A_{\mathrm{f}}\left(n_1 - \frac{d}{2}\right) \tag{1}$$

where E_{f} and A_{f} are for the flange the longitudinal modulus of elasticity and cross-sectional area. The moment distribution $M(x)$ along the length of the beam is given by

$$M(x) = k\sum_{i=1}^{3}(EI)_i + F\,(H-d) \tag{2}$$

where the summation (i = 1 to 3) is for the flexural rigidities of the web and flange components (the two identical webs used to form the closed box-section can be combined as a single component) assuming a state of non-interaction.

The strain difference e at the interface between web and flange is given by

$$e = k\left(\frac{H}{2} - d^*\right) - k\left(n_1 - d^*\right) = k\left(\frac{H}{2} - n_1\right). \tag{3}$$

Rearranging Equation (1) for unknown variable n_1 and substituting into Equation (3) the curvature is given by

$$k = 2\left(\frac{e + \dfrac{F}{E_{\mathrm{f}}A_{\mathrm{f}}}}{H-d}\right). \tag{4}$$

Substituting this new expression into Equation (2) gives, on rearranging, the following expression for the bending moment distribution

$$M(x) = \left(\frac{2\sum_{i=1}^{3}(EI)_i}{E_{\mathrm{f}}A_{\mathrm{f}}(H-d)} + (H-d)\right)F + \left(\frac{2\sum_{i=1}^{3}(EI)_i}{H-d}\right)e\,. \tag{5}$$

Let us now consider an element of length dx of the flange, as shown in Figure 4. The illustration shows a small length dx of the beam with the shear flow q (for convenience q in the figure includes the other half of the shear flow transfer from the second web). In reality the spacing Sp_x of the discrete connectors is many times bigger than dx; but for convenience we assume in the analytical treatment that the shear stiffness is uniformly smeared out. On the left side the resultant flange force is F and this has increased on the right side to F + dF. Because the element is in static equilibrium the longitudinal shear force per unit length is given by

$$q = -\frac{\mathrm{d}F}{\mathrm{d}x}. \tag{6}$$

To make a link to the shear stiffness provided by the method of connection we introduce the elastic shear stiffness of an individual connector. Stiffness K is defined as the force to cause unit slip between two components (e.g. flange and web) joined by a connector. Letting the connection spacing have distance Sp_x and the relative slip at the connection level be s, the elastic shear stiffness can be expressed as

$$K = \frac{q\,Sp_x}{s}. \tag{7}$$

Substituting Equations (7) and (6) into the relationship between slip s, and strain difference e, gives

$$e = \frac{\mathrm{d}s}{\mathrm{d}x} = \frac{Sp_x}{K}\frac{\mathrm{d}q}{\mathrm{d}x} = \frac{Sp_x}{K}\left(-\frac{\mathrm{d}^2F}{\mathrm{d}x^2}\right). \tag{8}$$

Equation (8) is substituted into Equation (5) to derive the governing second-order differential equation for $M(x)$ of a three-layered beam possessing partial shear interaction from having uniform spaced connector at two interfaces linked to the upper and lower flanges.

$$M(x) = \left(\frac{2\sum_{i=1}^{3}(EI)_i}{E_{\mathrm{f}}A_{\mathrm{f}}(H-d)} + (H-d)\right)F - \frac{Sp_x}{K_{\mathrm{s}}}\left(\frac{2\sum_{i=1}^{3}(EI)_i}{H-d}\right)\frac{\mathrm{d}^2F}{\mathrm{d}x^2} \tag{9}$$

Specific analytical solutions for different loading and end displacement cases can be developed from Equations (2) and (9) to obtain expressions for the flange resultant force F and the mid-span (vertical) deflection.

Our theoretical model will now be developed for the case of four-point bending, using the model shown in Figure 5. When loading and end boundary conditions are symmetrical the mid-span deflection is the maximum vertical deflection, which we shall defined as $v_{(\text{total})}$ for the combination of deflection contributions from bending ($v_{(\text{bending})}$) and shear. The co-ordinate system has the x-axis coincident with the beams longitudinal centroid axis and the y-axis is in the vertical plane (and positive is downwards); the variable for the beam's deflection is therefore $v(x)$. Similar solutions for other load cases (e.g., uniformly distributed and three-point bending) and simply supported ends can be readily derived using the same solution methodology. The justification for presenting the derivation of the equations for the case of four-point bending is that this was the loading case used by Evernden (2006) to characterize the partial shear interaction of the prototype beam introduced earlier in this paper.

For the beam in Figure 5 of total span length L, and having a load P at distance a from each free end, the bending moment $M(x)$ in Equation (9) is Px for $0 \le x \le a$ and $a + b \le x \le L$, and Pa in the mid-span constant moment region, given by $a \le x \le a + b$. To simplify the solution's algebra we define the two new parameters of

$$\psi = \sqrt{\frac{\beta}{\lambda}} \tag{10}$$

and

$$\phi = \frac{P}{\beta} \tag{11}$$

with $$\lambda = \frac{Sp_x}{K}\left(\frac{2\sum_{i=1}^{3}(EI)_i}{H-d}\right) \qquad \text{and} \qquad \beta = \frac{2\sum_{i=1}^{3}(EI)_i}{E_{\text{f}}A_{\text{f}}(H-d)} + (H-d).$$

Substituting in Equation (9) for the parameters ψ and ϕ (with Equations (10) and (11)), the second-order differential can be expressed as

$$\frac{\mathrm{d}^2F}{\mathrm{d}x^2} - \psi^2 F + \psi^2 \phi x = 0 \qquad \text{for } x \le a. \tag{12}$$

This differential equation has the solution

$$F = \overline{A}\cosh(\psi x) + \overline{B}\sinh(\psi x) + \phi x. \tag{13}$$

From inspection we can apply the boundary condition that $F = 0$ at $x = 0$, to establish $\overline{A} = 0$. Over the mid-span length region the moment is constant and, at $x = a$, we have the continuity boundary condition that $\frac{\mathrm{d}F}{\mathrm{d}x} = 0$. It follows that $\overline{B} = -\frac{\phi}{\psi \cosh(\psi L)}$. Introducing the constants into Equation (13) the flange resultant force varies along the left-hand length, to $x = a$, as

$$F_{x \le a} = \phi\left(x - \frac{\sinh(\psi x)}{\psi \cosh(\psi a)} \right) . \tag{14}$$

For x from a to $a + b$ there is no change in F and it takes the constant value given by

$$F_{a \le x \le a+b} = \phi\left(a - \frac{\tanh(\psi a)}{\psi} \right). \tag{15}$$

To obtain an expression for the vertical deflection we use Equations (14) and (15) to eliminate F from Equation (2) for the two different moment distributions existing along the beam's length. The resulting moment curvature equation for $0 \le x \le a$ is

$$\sum EI \frac{\mathrm{d}^2 v}{\mathrm{d}x^2} = \phi\left(x - \frac{\sinh(\psi x)}{\psi \cosh(\psi a)} \right)(H - d) - Px . \tag{16}$$

Integrating Equation (16) once with respect to x gives

$$\sum EI \frac{\mathrm{d}v}{\mathrm{d}x} = \phi\left(\frac{x^2}{2} - \frac{\cosh(\psi x)}{\psi^2 \cosh(\psi a)} \right)(H - d) - P\frac{x^2}{2} + \overline{C} \tag{17}$$

and integrating again with respect to x gives

$$\sum EIv = \phi\left(\frac{x^3}{6} - \frac{\sinh(\psi x)}{\psi^3 \cosh(\psi a)} \right)(H - d) - P\frac{x^3}{6} + \overline{C}x + \overline{D} . \tag{18}$$

Equations (16) to (18) are valid only for $x \le a$. For the mid-span section of the beam ($a \le x \le a + b$) the constant moment is Pa and this leads to Equation (16) having the terms

$$\left(\sum EI\right)\frac{\mathrm{d}^2 v}{\mathrm{d}x^2} = F_{a \le x \le a+b}(H - d) - Pa \tag{19}$$

To simplify the presentation, substitution of the expression for the constant F will be made after the integration process. Integrating twice with respect to x gives

$$\left(\sum EI\right)\frac{\mathrm{d}v}{\mathrm{d}x} = F_{a \le x \le a+b}(H - d)x - Pax + \overline{C}_{\mathrm{m}} \tag{20}$$

and

$$\sum EI\, v = F_{a\le x\le a+b}\,\frac{x^2}{2} - Pa\frac{x^2}{2} + \overline{C}_{\mathrm{m}}x + \overline{D}_{\mathrm{m}} \tag{21}$$

for the slope and deflection expressions, respectively. The subscript $_{\mathrm{m}}$ to the constants of integration is given because the mid-span constants cannot, respectively, be the same as $\overline{C}$ and $\overline{D}$ in Equations (17) and (18). Equations (19) to (21) are valid only for $x \le a + b$.

Boundary conditions for slope and deflection are required to establish the four constants of integration. At $x = 0$ the vertical deflection $v(0)$ is taken to be zero (for a suitable datum), and from Equation (18) this enforces $\overline{D} = 0$. The slope at mid-span is zero and slope in the mid-span section is given by Equation (20). Inserting $x = L/2$ into this expression gives

$$\overline{C}_m = P\left(\frac{aL}{2}\right) - (H-d)F_{a\le x\le a+b}\left(\frac{L}{2}\right). \tag{22}$$

Next the slope continuity at $x = a$ is used to equate Equations (17) and (20), and this gives

$$P\frac{1}{\beta}\left(\frac{a^2}{2} - \frac{1}{\psi^2}\right)(H-d) - P\frac{a^2}{2} + \overline{C} = a(H-d)F_{a\le x\le a+b} - P\,a^2 + \overline{C}_{\mathbf{m}}$$

that on rearranging establishes

$$\overline{C} = \left(F_{a\le x\le a+b}\left(a - \frac{L}{2}\right) - P\frac{1}{\beta}\left(\frac{a^2}{2} - \frac{1}{\psi^2}\right)\right)(H-d) - \frac{Pa^2}{2} + \frac{PaL}{2}. \tag{23}$$

To determine the fourth constant, $\overline{D}_{\mathrm{m}}$, we consider the continuity of vertical deflection at the supports ($x = a$), and equate Equations (18) and (21), to obtain

$$\phi\left(\frac{a^3}{6} - \frac{\tanh(\psi a)}{\psi^3}\right)(H-d) - P\frac{a^3}{6} + \overline{C}a = (H-d)F_{a\le x\le a+b}\,\frac{a^2}{2} - P\frac{a^3}{2} + \overline{C}_{\mathrm{m}}a + \overline{D}_{\mathrm{m}}. \tag{24}$$

On rearranging Equation (21) and substituting for $\overline{C}$ and $\overline{C}_{\mathrm{m}}$ the unknown integration constant in Equation (24) is

$$\overline{D}_{\mathrm{m}} = \left(P\frac{1}{\beta}\left(\frac{a}{\psi^2} - \frac{a^3}{3} - \frac{\tanh(\psi a)}{\psi^3}\right) + F_{a\le x\le a+b}\left(\frac{a^2}{2}\right)\right)(H-d) - P\frac{a^3}{6}. \tag{25}$$

The expression for the vertical deflection at mid-span ($x = L/2$) is given by

$$v_{(\mathrm{bending})} = \frac{1}{\sum EI}\left(\left[\frac{P}{\beta}\left(\frac{a}{\psi^2} - \frac{aL^2}{8} + \frac{a^3}{6}\right) + \frac{\tanh(\psi a)}{\psi}\left(\frac{L^2}{8} - \frac{a^2}{2} - \frac{1}{\psi^2}\right)\right](H-d) + P\frac{L^3}{6}\left(\frac{3a}{4L} - \left(\frac{a}{L}\right)^3\right)\right). \tag{26}$$

Substituting for, and expanding the terms $\overline{C}_m$, $\overline{D}_m$ and $F_{a\le x\le a+b}$, we obtain the expression for Equation (27), which is found to degenerate to the pure bending vertical displacement upper limit solution when parameter ψ tends to infinity.

$$v_{(\text{bending})} = \frac{1}{\sum EI}\left(\left[\frac{P}{\beta}\left(\frac{a}{\psi^2}-\frac{aL^2}{8}+\frac{a^3}{6}\right)+\frac{\tanh(\psi a)}{\psi}\left(\frac{L^2}{8}-\frac{a^2}{2}-\frac{1}{\psi^2}\right)\right](H-d)+P\frac{L^3}{6}\left(\frac{3a}{4L}-\left(\frac{a}{L}\right)^3\right)\right) \quad (27)$$

To calculate the total mid-span deflection the term for shear deformation is included. Finally, the equation for the maximum deflection is

$$v_{(\text{total})} = \frac{1}{\sum EI}\left(\left[\frac{P}{\beta}\left(\frac{a}{\psi^2}-\frac{aL^2}{8}+\frac{a^3}{6}\right)+\frac{\tanh(\psi a)}{\psi}\left(\frac{L^2}{8}-\frac{a^2}{2}-\frac{1}{\psi^2}\right)\right](H-d)+P\frac{L^3}{6}\left(\frac{3a}{4L}-\left(\frac{a}{L}\right)^3\right)\right)+\left(\frac{Pa}{G_{xy}A_v}\right) \quad (28)$$

where G_{xy} is the in-plane shear modulus of elasticity of the web material and A_v is the area of the section assumed to be resisting the shear force (Mottram, 1991; Bank, 2006).

2.1 Analytical study

Having solved the partial interaction problem for a three-layered beam subjected to four-point bending a numerical study is presented to indicate how beam performance indicators change with the degree of shear interaction achieved by using the same mechanical fasteners spaced equally at distance Sp_x. The pultruded FRP beam specimen shown in Figures 1(a) to 1(c) was assembled by Evernden (2006) from four pultruded components and Unistrut M10 fasteners. It has a total depth of 400 mm (H) and a total span (L) of 2846 mm and the nominal area of a flange (A_f) is 5540 mm^2. Properties of this experimental beam will be used to evaluate the closed form expressions (14) and (15) for the flange force F, and Equation (27) for the bending deflection $v_{(\text{bending})}$. For convenience the calculations are made with the vertical loading set to $2P$ = 20 kN. Table 1 gives the notation and the values of the physical properties (Evernden, 2006) used to obtain the numerical prediction plotted in Figures 6 to 7.

Figure 6 presents F from Equations (14) and (15) for various levels of connection flexibility to full-interaction (as defined by parameter Sp_x/K), against distance x from the left support to mid-span. It is evident from the curves in the figure that F increases from very low values, akin to the non-interaction state, to values close to that those for full-interaction, as Sp_x/K increases from 0.0001 to 1.0 mm^2/N. As required the

curves from the analytical solution give continuity in F at the internal support (at $x = a = 1016$ mm).

Plotted in Figure 7 is the change in maximum bending deflection, $v_{(\text{bending})}$, with increasing connection flexibility Sp_x/K between the lower and upper bound bending deflection limits of v_{non} and v_{full}. It is evident from the characteristics of the non-linear curves that the predictions from Equation (27) will tend to the upper limit as the state of complete non-interaction is approached. The finding raises the question, *What value of Sp_x/K would be optimum in practice?* Clearly, for the optimum design solution it is necessary to consider all relevant limit states towards both ultimate and serviceability modes of failure. The required states will, of course, depend on the chosen geometry and FRP material for the flange and web components, the type of connector, and the beam's displacement boundary conditions and design loading cases. Considering the low longitudinal modulus of elasticity of pultruded FRP (typically 23 GPa (Anon, 2010a)) compared to traditional construction materials (e.g. 210 GPa for structural steels and 70 GPa for Aluminium alloys), deflections are more likely to be the critical limit state, followed by an buckling instability and, maybe, yet less probable, material rupture (Bank and Mosallam, 1991; Mottram, 1991; Mottram, 1993; Bank, 2006).

When specifying the details for a 'flat-pack' box-beam it is reasonable that we should not want to specify a connection performance that causes the vertical deflection to be significantly higher than when the beam is in a state of full-interaction. The curve in Figure 7 shows that such a theoretical state of full-interaction is only achievable when $Sp_x/K \rightarrow 0$, and to provide such a joint flexibility by using mechanical fasteners is going to be neither economical nor practical. To be pragmatic, it is going to advisable to set an upper limit to the degree of shear interaction, accepting a certain loss in beam stiffness due to the method of connection employed. It should be noted that a small increase in connection flexibility Sp_x/K, from zero, can produce a dramatic increase in maximum bending deflection. It is likely that the flat-pack concept would not be fit for intended use if the deflection exceeded double the full interaction minimum. This condition will be achieved with the prototype beam when $Sp_x/K \leq 0.0061$.

We have therefore discovered that in order to have a box-section, using mechanical fasteners to connect the components for the closed shape, we will have to balance the needs for maximum flexural stiffness, against cost and buildability. It should further be understood that there are going to be limits set upon connector spacing Sp_x, the lower value specified to avoid group connector interaction and the upper value of connector spacing to prevent a local buckling failure between two fastener positions in the compression zone.

3.0 Comparison of analytical modeling with experimental results

To be able to compare the performance of the closed form equations from the analytical treatment with what can occur in practice there are the measured values of interface slippage and vertical beam deflections from a series of tests by Evernden (2006), using the prototype beam specimen shown in Figure 1. Span L is 2846 mm and the distance (a) from a load P to a simple supports is 1016 mm. To vary the degree of interaction between the flange and web components changes were made to the number M10 Unistrut connectors and their spacing distances (via Sp_x) along the length of the four interfaces. Symmetry in the connector layout about the mid-span was maintained and so the number of Unistruts and their spacings are the same along the four web/flange interfaces.

Evernden and Mottram (2007) have presented an evaluation of the flexural behaviour of the prototype beam in Figure 1, covering four different connection layouts from the PhD study. For purposes of this paper the experimental responses of these four assemblies, given the labels BA-A50-AP, BA-A100-AP, BA-A200-AP and BA-A400-AP (Evernden, 2006; Evernden and Mottram, 2007), will be considered. For identification of a beam the term 'BA' refers to Beam Assembly, 'A50' indentifies that the specimen is tested with load Arrangement A (shown in Figure 5) and has connections at a constant spacing (Sp_x) of 50 mm, and 'AP' indicates that both *active* and *passive* connections are present (i.e. connectors are uniformly spaced along the entire interface lengths). If connections were confined to the side shear spans the last term would be given as (A) indicating only *active* connections.

An expression for the theoretical total deflection of a shear deformable beam (Timoshenko, 1955) has the general form of

$$v_{(\text{total})} = \mathrm{C}_1 \frac{PL^3}{EI} + C_2 \frac{PL}{G_{xy} A_v}. \tag{29}$$

The mid-span deflection $v_{(\text{total})}$ depends upon the total applied load P, the span length L, the section flexural modulus of elasticity E, the second moment of area about the axis of bending I, the shear area A_v and the section shear modulus of elasticity G_{xy}. Constants C_1 and C_2 depend upon the load and displacement boundary conditions. For the specific case of four-point bending under a total load of $2P$ (see Figure 5) the total deflection involves distance a measured from a loading location to the simple end support. For the prototype beam the total deflection using Timoshenko beam theory is

$$v_{(\text{total})} = \frac{1}{EI}\left(P\frac{L^3}{6}\left(\frac{3a}{4L} - \left(\frac{a}{L} \right)^3 \right) \right) + \frac{Pa}{G_{xy} A_v}. \tag{30}$$

By taking values of EI that represent the states of full-interaction (in which all element in the assembly act as a single element without slip) and the state of non-interaction (in which the elements act individually) into Equation (30) the theoretical upper and lower bounds of the beam's mid-span deflection are obtained. From Table 1 these flexural rigidities are $EI_{\text{full}} = 5.6\times10^{12}$ N/mm^2 and $EI_{\text{non}} = 9.6\times10^{11}$ N/mm^2, respectively. In the calculation of EI_{full} a transformed section is required to account for the difference in longitudinal tensile modulus of the web and flange materials being 16.2 GPa (Lutz, 2004) and 24 GPa (Lane, 2002), respectively. The in-plane shear modulus G_{xy} for flat sheet material resisting the shear force may reasonably we taken to be 4 GPa, following the evaluation by Mottram (2004). For the properties of the prototype beam given in Table 1 or reported elsewhere in this paper it is found that the contribution of shear deformation to the total deflection ($v_{(\text{total})}$) is 26% and 6% for full- and non-interaction, respectively.

These bounding flexural rigidities give the linear curves in Figure 8, with the bold solid line for the full-interaction case and the bold dashed line for the non-interaction situation. The experimental P v $v_{(\text{total})}$ plots, lying between the bounds, enable us to compare the beam's relative stiffness for the four different connection layouts, which can be established from the gradients to the curves.

It is important to understand that, from a critical evaluation of his test results, Evernden (2006) discovered that secondary effects, such as out-of-plane deformations resulting from geometric imperfections, interacted with the primary vertical deformations ($v_{(total)}$) that the equation presented herein predict. This finding is supported by research results from Roberts and Masri (2003) and Hayes and Lesko (2004), who independently identified that 'so-called' secondary effects can be significant (and difficult to extricate) when the purpose of experiments is to establish the flexural properties of a FRP beam. It is therefore not feasible to compare the PhD measurements for $v_{(total)}$ (Evernden, 2006) directly with analytical predictions using Equation (28).

It is instructive to summarize the findings from the theoretical and experimental results plotted in Figure 8. The shape of a load-deflection (P v $v_{(total)}$) curve from testing appears to be dependent on the spacing of the Unistruts. For the two layouts BA-A50-AP (--♦--) and BA-A100-AP (--x--) with connection spacing Sp_x set at 50 and 100 mm specimens, the P-$v_{(total)}$ relationship may be taken to be approximately linear, while it should be approximated to a bi-linear response for the two lay-outs BA-A200-AP (--○--) and BA-A400-AP (--□--) when the constant connection spacings is higher, at 200 and 400 mm, respectively. It is noteworthy that the test results in Figure 8 for the spacing of 100 mm indicate that the prototype beam is giving an acceptable degree of interaction. For the reason given later the value of Sp_x/K remains unknown. When P is 20 kN the total deflection was measured to be 20% higher than for the theoretical full-interaction situation. An in-depth assessment and evaluation on the behavior of the prototype beam shown in Figure 1 is given in Evernden (2006). One observation from the plots in Figure 8 of an increase in the apparent flexural stiffness with increasing number of connections is to be expected.

It is possible to make an assessment of the theoretical solution given by Equation (28) through the process of back substitution utilising the load-slip (P v s) results presented in Figure 9. The slip displacement in this figure is the relative movement between a flange and web measured at a beam's end. Using any curve in Figure 9 for a beam lay-out the mean shear force per connector can be determined, from which an effective stiffness K per unit length can be estimated at each load increment (load sates are given by the symbols on the four experimental curves). By now substituting

this K into Equation (28), by way of parameter λ, we can obtain the mid-span bending deflection that accounts for a state of partial interaction. The mid-span contribution due to shear deformation is given by the last term in Equation (28).

Plotted in Figure 10 are these total vertical deflections ($v_{(total)}$) for the four constant connector spacings of 50, 100, 200 and 400 mm. The general trend shows an increase in flexural stiffness with increasing number of connectors and the four semi-empirical curves all fall within the theoretical upper and lower bounds for full- (EI_{full}) and non-interaction (EI_{non}). With the exception of the single case, having Sp_x = 400 mm, the other three load-deflection curves exhibit a highly non-linear response, each with an initially relatively high stiffness, followed by an ever decreasing stiffness that tends towards the lower stiffness for the lower bound condition of non-interaction. Upon initial loading the shear deformation contribution to the total defection is calculated to be 25 and 20 percent for the upper and lower bounds of interaction. These percentages reduce to lie within the range of 22 to 10 percent as the assemblies are loaded to P = 20 kN, as they exhibit a state of growing partial interaction. As K for a connection lay-out is derived from the experimental results in Figure 9 the equivalent connection lay-out curve in Figure 10 follows a similar shape. However the analytical predictions in Figure 10 show an increase in $v_{(total)}$ of between 10 and 38 percent. This finding may be accounted for by considering the reliability of the experimentally determined deflections and slippages. As noted above these displacements had to be derived from measurements that included significant secondary effects that cannot easily be extricated to obtain, in isolation, the 'theoretical' beam response that the analytical modelling assumes.

As found by Evernden and Mottram (2007) the assumption of a constant K for the M10 Unistrut (at 2.5 kN/mm for a tightening torque of 20 Nm) is inappropriate because the slip measurement used to determine this connector shear stiffness (Evernden & Mottram, 2006) is different to that experienced in the prototype beam. K = 2.5 kN/mm was calculated using the mean load-slip response, from a batch of six non-standard pull-out test specimens, shown in Figure 2, to a slip of 1.0 mm. Given the lower values of s in Figure 9, its maximum is 0.5 mm, the choice by Evernden and Mottram (2006) to take more than double this practical slip when determining K is

one plausible reason why we have significantly underestimated the actual shear stiffness when the prototype beam is deformed.

The shear force with slip curve given in Figure 2(c) is representative of a Unistrut connector's behaviour in the pull-out test to slips up to 0.5 mm (Evernden and Mottram, 2006). Stiffness K can be taken as its secant gradient, at the level of slip required to correspond to the slip in testing. The family of P v $v_{(total)}$ curves in Figure 11 are calculated using the representative K for each load step determined from the pull-out test results in Figure 2(c). The general trend for the four connection lay-outs is non-linear with the expected increase in flexural stiffness with reduced connector spacing from 400 to 50 mm. The four curves are again bounded by the full- and non-interaction theoretical limits given by the bold solid and bold dashed lines, respectively. Each curve exhibits an initially higher beam stiffness that, with deflection, decreases non-linearly until the final stiffness (for $v_{(total)}/L > 1/300$) is similar to the non-interaction stiffness. As the flexural stiffness of the assemblies decrease with P so does the shear deformation contribution to the total deflection reduce from initial between 13 and 10 percent to, at P = 20 kN, between 10 and 6 percent. More importantly, it is observed that the analytical deflections for $v_{(total)}$ in Figure 11 are higher than the measured deflections for $v_{(total)}$ given in Figure 8. This comparison suggests that the representative mean connector load-slip curve from the pull-out test method (Evernden and Mottram, 2006) provides a significant underestimate to the real longitudinal shear stiffness that exists in the four prototype beam assemblies.

Comparing the equivalent load-deflection curves in Figures 10 and 11 it is apparent that the representative K is lower than that determined from the measured interfacial slip. This is an interesting result given that the latter method of determination should give the higher value, since it involves the effect of frictional forces between the contacting flange and web components. In other words this study finds that the actual connection flexibility (Sp_x/K) is not solely due to the number and spacing of the M10 Unistruct connectors. From the study reported in this paper it is shown that the non-standard test method by Evernden and Mottram (2006) for the determination of K is not ideal. Finally, it can be noted that for the purpose of demonstrating that the

analytical model developed in this paper can be used (see Figure 11) the representative stiffness of the connector (from Figure 2(c)) is found to be acceptable.

4.0 Concluding Remarks

Modifying the well-known Newmark method for partial shear interaction in two-layered beams (Newmark *et al*., 1952) the authors formulate new closed formed expressions for analyzing box-beams having shear interaction at the two interfaces between two parallel webs and the upper and lower flanges they are connected to. Expressions for the resultant flange force and mid-span vertical deflection are presented for the single load case of four-point bending.

Using properties for a prototype box-beam fabricated of pultruded fiber reinforced components and having M10 Unistrut connectors for the method of connection, the closed form solutions for the flange force and vertical deflection are shown to converge to the upper and lower bound limits given by the interaction states of full- and non-interaction. The analytical treatment is found to provide us with predictions of beam performance towards establishing the connection flexibility needed to achieve a given level of interaction. Knowing the shear stiffness from different methods of connections it will be feasible to use the closed form equations in this paper to aid in the design of 'flat-pack' box-beams with higher flexural rigidities (deeper sections) than can be sourced today from the range of single pultruded profiles (see Anon, 2010a; Anon 2010b; Anon 2010c).

Through the comparison of results from the analytical modeling and prototype beam testing (Evernden 2006) it has been shown herein that Equation (28) for the total vertical deflection can be used providing the connection shear stiffness is that present at the interfaces in the beam assembly. Because this stiffness has been found not to be what is measured by using the non-standard pull-out test method created Evernden and Mottram (2006) it is concluded that a suitable test methodology for determining connector shear stiffness is required.

References

Anon. (2010a). *The New and Improved Pultrex® Pultrusion Design Manual (Imperial Version)*, Creative Pultrusions, Inc., Alum Bank, PA.
//www.creativepultrusions.com/rd.html (Literature library) 20 August 2010.

Anon. (2010b). *Strongwell Design Manual*, Strongwell, Bristol, VA.
//www.strongwell.com/ (Literature) 20 August 2010.

Anon. (2010c). *Fiberline Design manual*, Kolding, Denmark //www.fiberline.com/ 20 August 2010.

Anon. (2003). *EXTREN DWB® design guide*, Strongwell, Bristol, Va.

Lane A. (2002). *An experimental investigation of buckling mode interaction in PFRP columns*, PhD thesis, University of Warwick, UK.

Bank, L. C. and Mosallam, A. S. (1991). Linear and nonlinear response of pultruded FRP frames subjected to static loads, *Symposium on Plastics and Plastic Composite: Material Properties, ASME Winter Annual Meeting*, Atlanta, Georgia, pp. 1-6.

Bank, L. C. (2006). Composites for Construction - Structural Design with FRP Materials, John Wiley & Sons, NJ.

Evernden, M.C. (2006). *Structural evaluation of a novel box-beam system of pultruded FRP shapes*, PhD thesis, University of Warwick, UK.

Evernden, M.C. and Mottram, J. T. (2006). Characterization of Unistrut connection method with pultruded fiber reinforced polymer channels, *Journal of Materials in Civil Engineering,* **18** 5, 700-709.

Evernden, M.C. and Mottram, J. T. (2007). Theoretical and experimental analysis of a modular PFRP box-beam concept constructed of separate plate elements and mechanical fasteners, *In*: *Proceedings 3rd International Conference on Advanced Composites in Construction,* ACIC07, York Publishing Services Ltd., York, 2007, 379-388.

Hayes, M.D. & Lesko, J.J. (2004). The effect of non-classical behaviours on the measurement of the Timoshenko shear stiffness, *in Proceedings 2nd International Conference on FRP Composites in Civil Engineering,* CICE 2004, Taylor and Francis Group, London, 873-880.

Johnson, R. P. (2004), *Composite structures of steel and concrete: Beams, slabs, columns, and frames for buildings*, Blackwell Publications, Malden, MA.

Lee, Y. J., Boothby, T. E. and Nanni, A. (1999). Slip modulus of FRP sheets bonded to concrete, *ACI Structural Journal*, **2** 95, 142-152.

Lutz, C. (2005). *Structural integrity of bolted joints for PFRP profiles*, PhD thesis, University of Warwick, UK.

Mottram, J. T. (1991). Structural properties of a pultruded E-glass fibre-reinforced polymeric I-beam, *In: Proceedings 6th International Conference on Composite Structures*, Elsevier Applied Science, (1991), 1-28.

Mottram, J. T. (1993). Recommendations for the optimum design of pultruded frameworks, *Mechanics of Composite Materials*, **29** 5, 675-682.

Mottram, J. T. (2004). Shear modulus of standard pultruded FRP material, *J. Composites for Construction*, **8** 2, 141-147.

Mottram, J. T. and Johnson, R. P. (1990). Push tests on studs welded through profiles steel sheeting, *The Structural Engineer,* **68** 10, 187-193.

Newmark, N. M., Siess, C. P. & Viest, I. M. (1952). Test and analysis of composite beams with incomplete interaction. *Proceedings of the Society of Experimental Stress analysis,* 1, 75 – 92.

Oehlers, D. J. and Bradford, M. A. (1995). *Composite steel and composite structural members – Fundamental behavior*, Elsevier Science, Amsterdam and San Diego, CA.

Rasheed, H. A. and Pervaiz, S. (2002). Bond slip analysis of fiber-reinforced polymer-strengthened beams, *Journal of Engineering Mechanics*, **128** 1, 78-86.

Roberts, T.M. & Masri, H.M.K.J.A.H. (2003). Section properties and buckling behavior of pultruded FRP profiles, *Journal of Reinforced Plastics and Composites* **22** 14, 1305–1317.

Timoshenko, S. (1955). *Strength of materials; Part 1: Elementary theory and problems*, Van Nostrand, New York.

Yam, L. C. P. (1981). *Design of composite steel-concrete structures*, Surrey University Press, Guildford, UK.

Table 1. Physical properties of prototype box-beam studied by Evernden (2006).

Physical Property	Notation	Value and units
Longitudinal Modulus of Elasticity of Flange material (from Lane, 2004)	E_f	24.0 kN/mm^2
Longitudinal Modulus of Elasticity of Web material (from Lutz, 2005)	E_w	16.2 kN/mm^2
Second moment of Area (full-interaction)	I_{full}	2.32×10^8 mm^4
Second moment of Area (non-interaction)	$\sum_{i=1}^{3} I$	4.00×10^7 mm^4
Area of flange section	A_f	5540 mm^2
Shear area (two webs)	A_v	4826 mm^2
Vertical separation of the two flange centriods	H-d	310 mm
Simply supported span	L	2846 mm
Shear span	a	1016 mm

Figure captions

Figure 1. (a) Prototype box-beam assembly with the Warwick University four-point bending test arrangement (from Evernden, 2006); (b) Prototype beam in assembly (c) Cross-section of prototype beam giving key dimension in millimeters; (d) M10 Unistrut steel connector.

Figure 2. (a) Load-slip test specimen and steel loading yoke; (b) Load-slip specimen in Dartec 9500 testing machine and subjected to tension loading; (c) Plot of representative slip (s) in mm with shear force for a M10 Unistrut connector.

Figure 3. Strain distributions in a three-layered cross-section with partial interaction.

Figure 4. Forces for a flange element of length dx.

Figure 5. Load case for four-point bending with lengths a and b defined.

Figure 6. Plots of resultant force in flanges with distance x for various joint flexibility Sp_x/K, with a = 1016 and b =814 mm in the four point bending experiments.

Figure 7. Plot of bending deflection with joint flexibility Sp_x/K.

Figure 8. Plots of total deflection with average load P for the prototype beam and with different connection stiffnesses.

Figure 9. Plots of connection slippage with average load P and with different connection stiffnesses.

Figure 10. Plots of load against total deflection from Equation (28) based on experimentally recorded interface slips from Figure 9.

Figure 11. Plots of load against total deflection from Equation (28) based on connector stiffness using the pull-out test results in Figure 2(c).

Figure 1

(a)

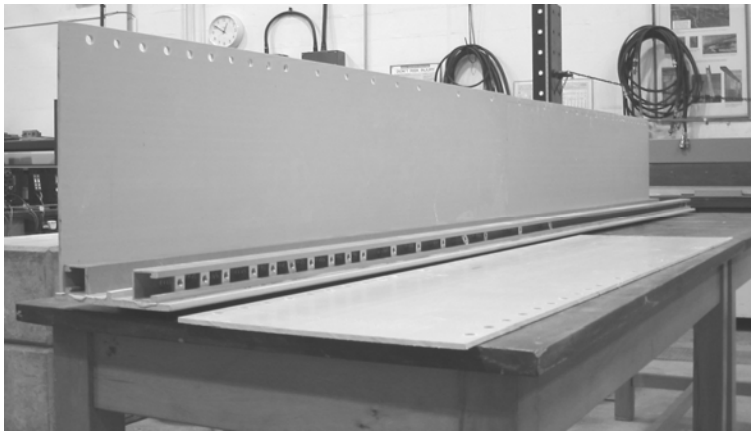

b)

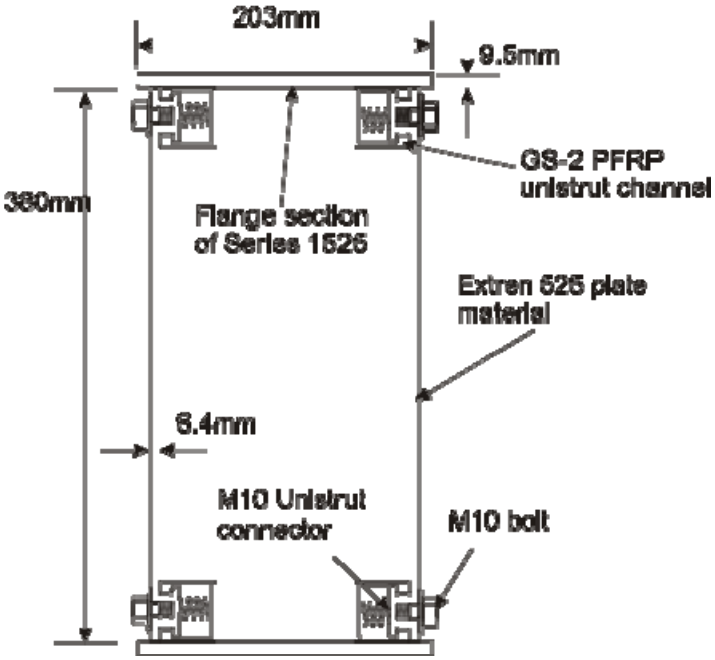
203mm
9.5mm
380mm
GS-2 PFRP
unistrut channel
Flange section
of Series 1525
Extren 525 plate
material
6.4mm
M10 Unistrut
connector
M10 bolt

(c)

(d)

Figure 2

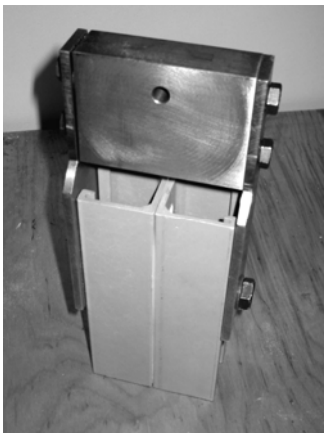

(a)

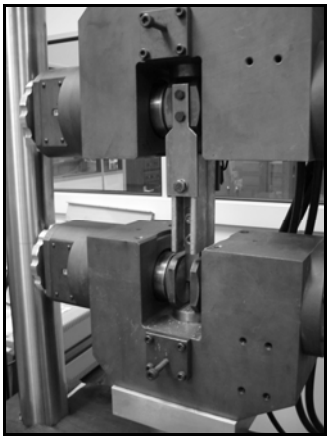

(b)

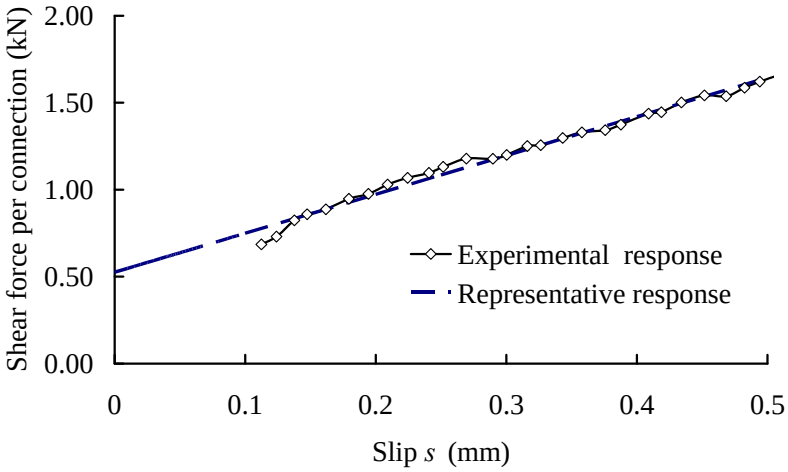
Shear force per connection (kN)
2.00
1.50
1.00
0.50
0.00
0
0.1
0.2
0.3
0.4
0.5
Slip s (mm)
Experimental response
Representative response

(c)

Figure 3

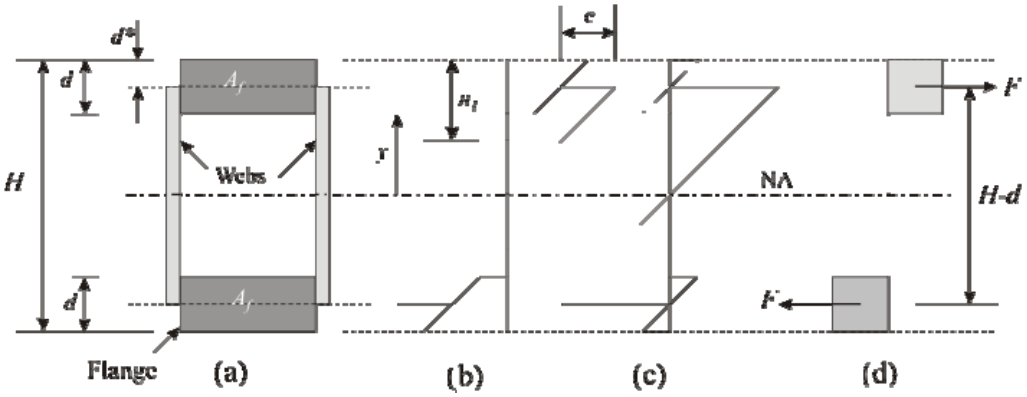

Figure 4

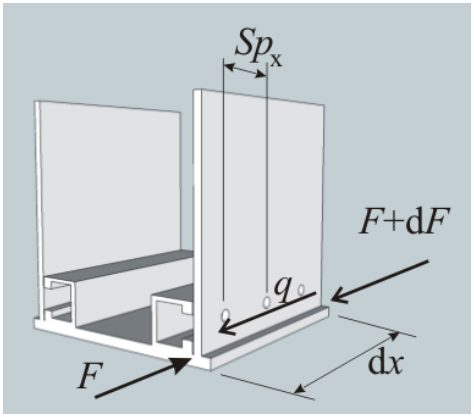

Figure 5

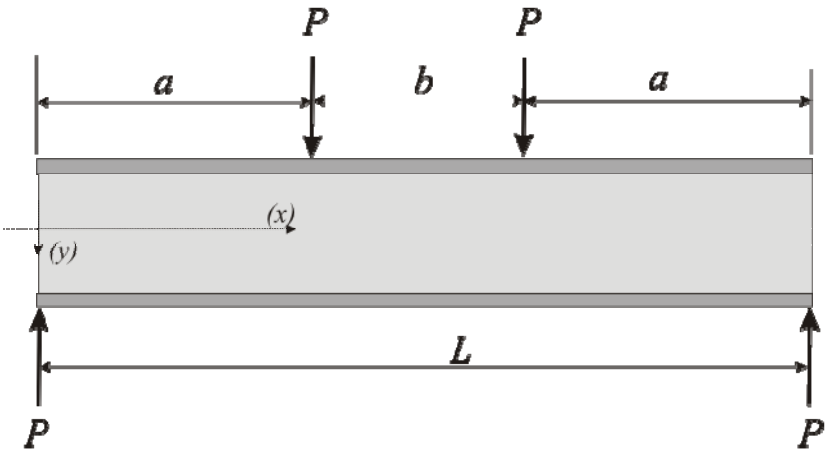

Figure 6

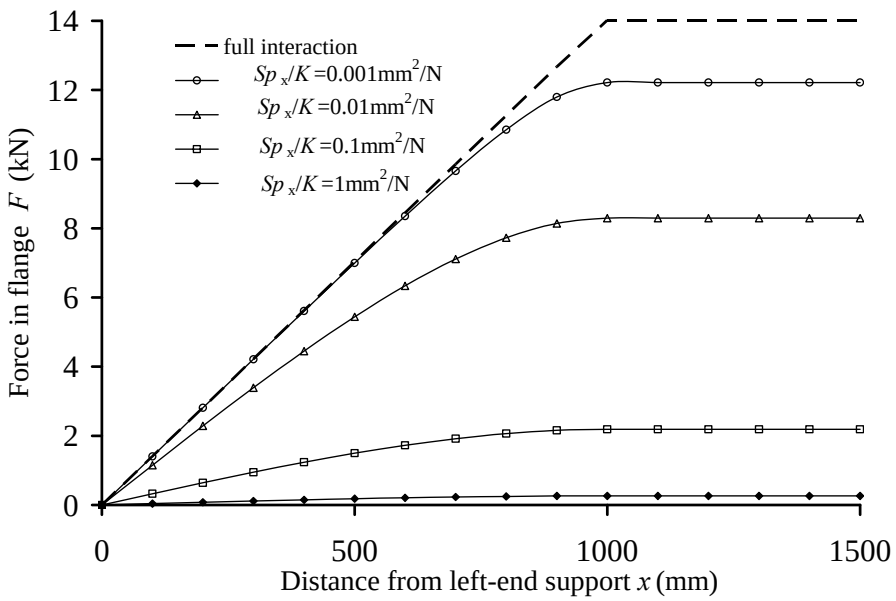
full interaction
Sp_x/K =0.001mm^2/N
Sp_x/K =0.01mm^2/N
Sp_x/K =0.1mm^2/N
Sp_x/K =1mm^2/N
Force in flange F (kN)
Distance from left-end support x (mm)
0
2
4
6
8
10
12
14
0
500
1000
1500

Figure 7

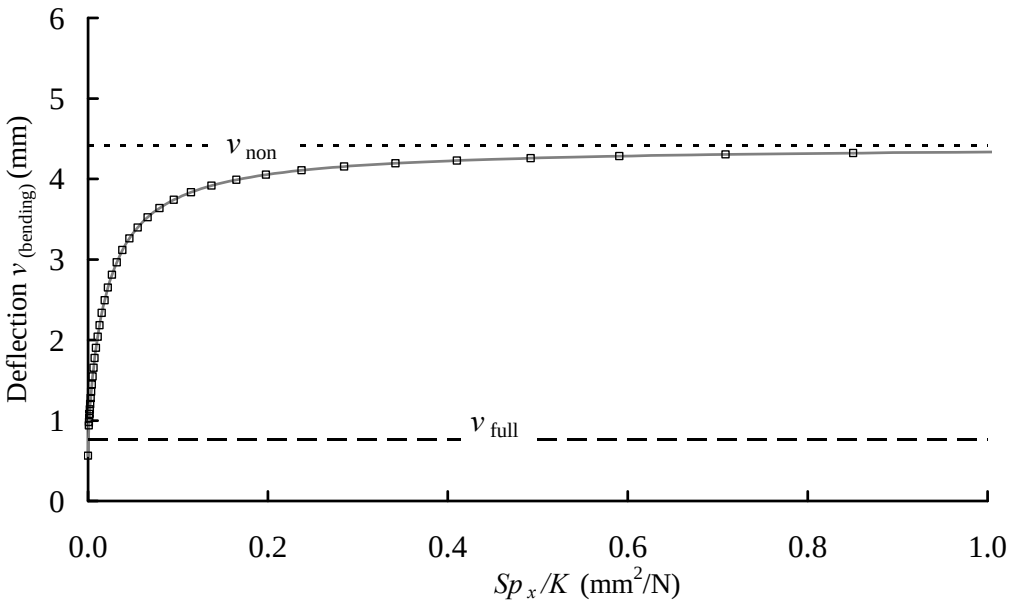
6
5
4
3
2
1
0
Deflection $v_{(bending)}$ (mm)
v_{non}
v_{full}
0.0
0.2
0.4
0.6
0.8
1.0
Sp_x/K (mm^2/N)

Figure 8

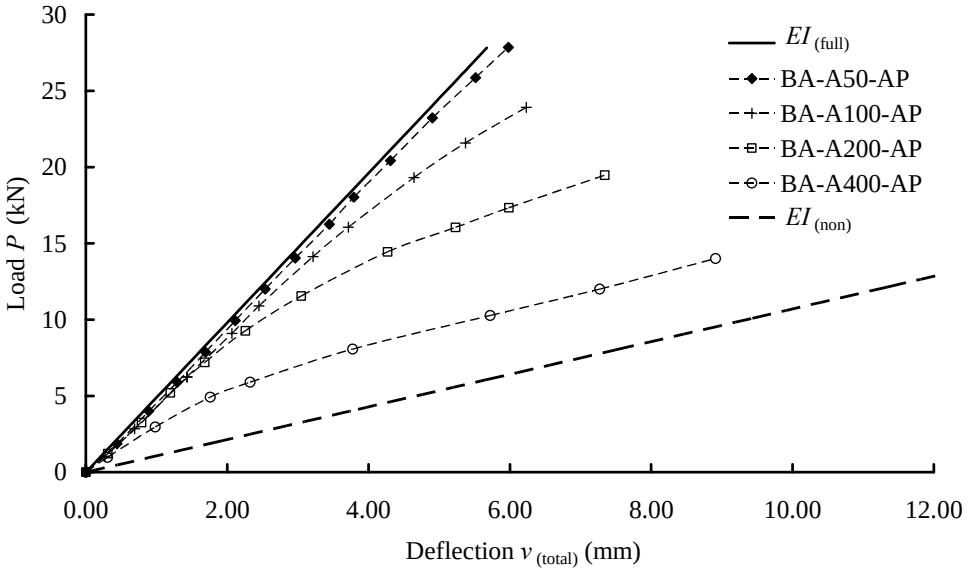
30
25
20
15
10
5
0
Load P (kN)
0.00
2.00
4.00
6.00
8.00
10.00
12.00
Deflection v (total) (mm)
EI (full)
BA-A50-AP
BA-A100-AP
BA-A200-AP
BA-A400-AP
EI (non)

Figure 9

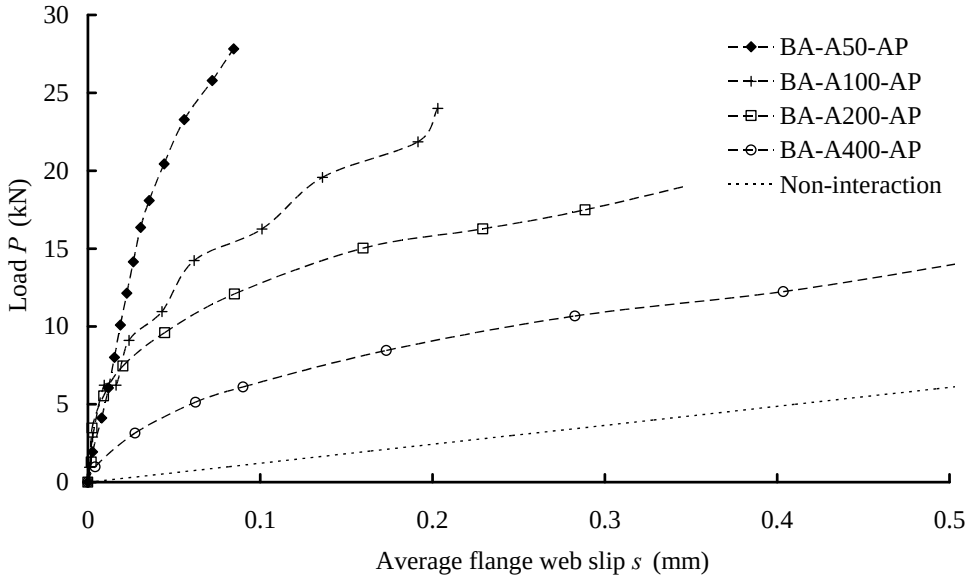

Figure 10

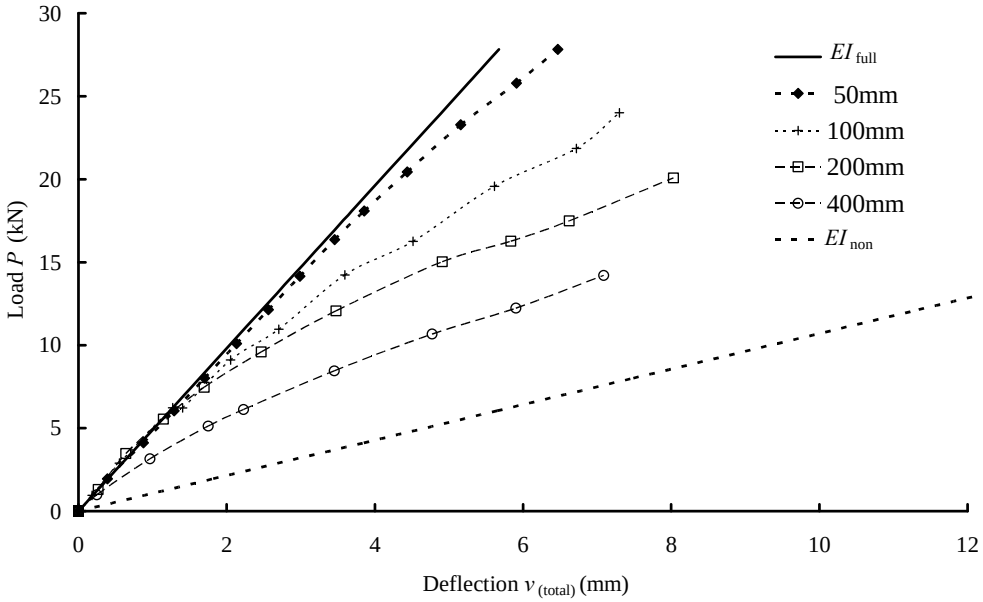

Figure 11

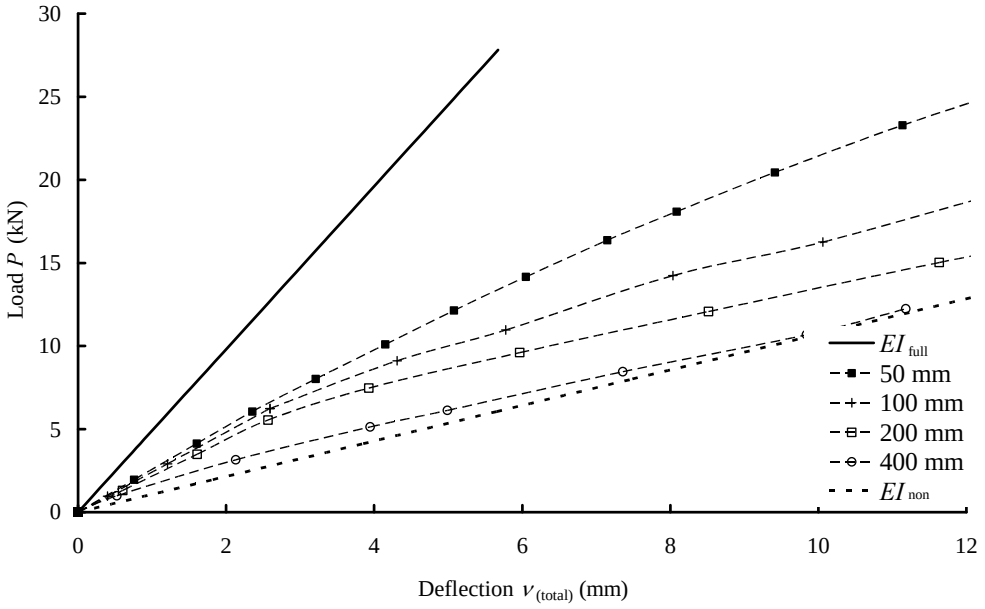
30
25
20
15
10
5
0
Load P (kN)
0
2
4
6
8
10
12
Deflection $v_{(total)}$ (mm)
EI_{full}
50 mm
100 mm
200 mm
400 mm
EI_{non}